Hydrodynamic Theory of Forced Dewetting

Jens Eggers

School of Mathematics, University of Bristol, University Walk, Bristol BS8 1TW, United Kingdom

(Received 24 December 2003; published 26 August 2004)

A prototypical problem in the study of wetting phenomena is that of a solid plunging into or being withdrawn from a liquid bath. In the latter, dewetting case, a critical speed exists above which a three-phase contact line is no longer sustainable and the solid can no longer remain dry. Instead, a liquid film is being deposited on the solid. Demonstrating this transition from a dry to a wetted solid to be of hydrodynamic origin, we provide the first theoretical explanation of a classical prediction due to Derjaguin and Levi: instability occurs when the outer, static meniscus approaches the shape corresponding to a perfectly wetting fluid. Our analysis investigates the conditions under which the highly curved contact line region can be matched to the static profile far away from it.

DOI: 10.1103/PhysRevLett.93.094502 PACS numbers: 47.20.Ma, 47.15.Gf, 83.50.Lh

The forced wetting or dewetting of a solid is an important feature of many environmental and industrial flows. In typical applications such as painting, coating, or oil recovery it is crucial to know whether the solid will be covered by a macroscopic film or not. If a solid is being withdrawn from a liquid bath (dewetting, see Fig. 1), a contact line is observed only for low speeds, in which case the solid remains dry (top diagram). If, however, a critical speed U_c is exceeded [1,2] (typically a few cm/sec), the contact line is no longer stable and a *macroscopic* film is deposited on the solid (bottom diagram). This is in marked contrast to a solid *plunging* into a liquid (wetting), in which case the velocity can be quite high (m/sec), while still maintaining a contact line [3].

The thickness of the wetting film shown in the bottom diagram of Fig. 1 is set by a balance of viscous forces and surface tension, which counteracts the viscous pull, as described 60 years ago by Landau, Levich, and Derjaguin (LLD) [4,5]. Lowering the speed once more, the LLD film is sustained down to much lower speeds than U_c until the film thickness corresponds to the range of intermolecular forces [2]. In this Letter, we will present a quantitative theory for the maximum speed U_c for which the solid can remain dry, based on a detailed description of the flow near the three-phase contact line.

It is well known [6,7] that viscous forces become very large near a moving contact line, and are controlled only by some microscopic cutoff λ, for example, a slip length [6,8]. As a result of the interplay between viscous and surface tension forces, the interface is highly curved, and the interface curvature κ at the contact line is set by λ^{-1} and increases with speed. The contact line speed U is properly measured by the capillary number $\mathrm{Ca} = U\eta/\gamma$, where η is the viscosity of the fluid and γ the surface tension between fluid and gas. Below we will show that $\kappa \propto \mathrm{Ca}^{1/3}/\lambda$.

Away from the contact line, on the other hand, viscous forces are negligible, and the meniscus shape is set by the competition between surface tension and gravity [4,5]. The scale of this static profile is thus set by the capillary length, $\ell_c = \sqrt{\gamma/(\rho g)}$, and its shape is determined by the *apparent contact angle* θ_{ap} the interface makes with the solid on a macroscopic scale. If the solid is at rest, θ_{ap} is the same as the equilibrium angle θ_e at the three-phase contact line between liquid, solid, and gas [9]. If the solid is however pulled away from the liquid, interface bending causes the angle θ_{ap}, measured macroscopically, to fall below θ_e.

It was first proposed by Derjaguin and Levi [10], and later reiterated by others [11], that the contact line disappears if θ_{ap} reaches *zero*. This notion was confirmed

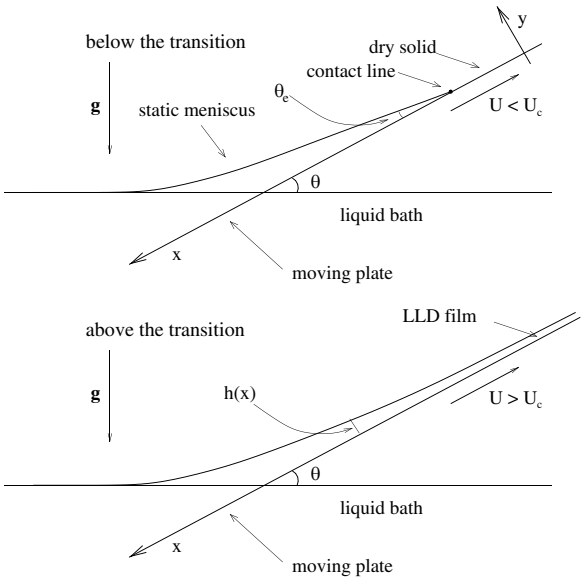

FIG. 1. A plate is being withdrawn from a liquid bath with speed U at an angle θ. If the speed is below a critical value U_c, the fluid forms a contact line with the solid, at which the slope of the interface is θ_e. Above U_c, the solid is wetted by a macroscopic film, whose thickness is governed by the classical theory of Landau, Levich, and Derjaguin (LLD) [4,5].

 0031-9007/04/93(9)/094502(4)$22.50

experimentally [1] by measuring the height of the meniscus around a fiber being withdrawn from a liquid. Another important set of experimental observations [12] was performed by displacing fluids of different viscosities and equilibrium contact angles θ_e from a capillary tube by pushing air into the tube: below a critical speed the tube was left dry, above it a fluid film was deposited on the walls of the tube. It was found that this critical speed corresponds to Ca/θ_e^3 exceeding a critical value, strongly pointing to a *hydrodynamic* mechanism for the instability.

In this Letter, we show that the existence of the contact line is determined by the interplay between the small-scale fluid motion near it (contact line region), and the static interface profile away from it (static region). Namely, the interface profile of the contact line region has to match onto the static profile, whose curvature is of order ℓ_c^{-1}. Since the curvature of the contact line region increases with speed, above a critical capillary number the contact line curvature will be too high for such a matching to be possible. This argument will enable us to explain the Derjaguin-Levi criterion of vanishing apparent contact angle from fundamental hydrodynamic principles.

We now turn to the geometry of Fig. 1 in more detail, but for the purpose of mathematical analysis restrict ourselves to the case of small angles θ and θ_e. In this regime of small slopes, the equations of motion simplify considerably, since the flow field can be effectively eliminated from the problem [9,13], leading to an equation for the thickness $h(x)$ (see Fig. 1) of the fluid film alone. It is well appreciated that this so-called lubrication approximation works very well in describing the interface profile near the contact line, faithfully describing experiments up to angles of about 100° [14].

To relieve the corner singularity at the moving contact line, we allow the fluid to slip across the solid surface, using the Navier slip law [8]

$$u|_{y=0} - U = \lambda \frac{\partial u}{\partial y}\bigg|_{y=0} \tag{1}$$

at the plate. The resulting lubrication equation for the interface shape $h(x)$ then is [13]

$$\frac{3\mathrm{Ca}}{h^2 + 3\lambda h} = h''' - h' + \theta, \tag{2}$$

where we consistently used the small-angle approximation $\tan(\theta) \approx \theta$, and lengths are nondimensionalized with the capillary length ℓ_c.

The left hand side of (2) corresponds to viscous forces, diverging as the contact line position $h(0) = 0$ is approached, but weakened by the presence of slip. Close to the contact line, viscous forces are balanced by surface tension forces (first term on the right), resulting in a highly curved interface near the contact line. The other two terms stem from gravity and only come into play at greater distances. As the simplest possible case, we also assume that the *microscopic* angle at the contact line $h'(0) = \theta_e$ is *independent* of speed. Far away from the interface, the surface coincides with that of the liquid bath, so the third boundary condition is $h'(\infty) = \theta$.

We now examine the contact line region and the static region in turn, to investigate the conditions under which they can be matched. Near the contact line, where h is small and the interface is highly curved, the left hand side of (2) is balanced by the first term on the right. Momentarily forgetting about slip as well, (2) reduces to

$$h''' = 3Ca/h^2, \tag{3}$$

whose solution can be expressed in terms of Airy functions [15]. This exact solution provides us with the key to understanding the fundamental difference between the case $\mathrm{Ca} > 0$, investigated here, and $\mathrm{Ca} < 0$, which would correspond to the solid *plunging* into the liquid. Namely, if $\mathrm{Ca} < 0$ (wetting), (3) has a solution whose curvature vanishes for $x/\lambda \gg 1$, so it can be matched onto the static solution. If, on the other hand $\mathrm{Ca} > 0$ (dewetting), the interface curvature predicted by (3) cannot fall below a lower bound. If this lower bound becomes too large as speed increases, the outer (static) meniscus can no longer accommodate the mismatch in curvature, and the contact line must disappear.

Namely, dewetting solutions of (3) (i.e., $\mathrm{Ca} > 0$) maintain a *finite* curvature $h''(x)$ at large distances $x/\lambda \gg 1$ from the contact line [15]:

$$\kappa_\infty = (3\mathrm{Ca})^{1/3}\left(\frac{2^{1/6}\beta}{\pi \mathrm{Ai}(s_1)}\right)^2 > 0, \tag{4}$$

where s_1 is the largest root of

$$\alpha \mathrm{Ai}(s_1) + \beta \mathrm{Bi}(s_1) = 0, \tag{5}$$

and Ai, Bi are Airy functions.

The constant β can be determined by matching the solution of (3) to the cutoff region $x \approx \lambda$, where one finds $h'(x) \approx [9\mathrm{Ca}\ln(\pi/(2^{2/3}\beta^2 x))]^{1/3}$. Comparing this to the first order expansion of the full Eq. (2) near the contact line [8,16],

$$h'(x) = \theta_e - \frac{3\mathrm{Ca}}{\theta_e^2}[1 + \ln(x\theta_e/\lambda)], \tag{6}$$

we find $\beta^2 = (\theta_e/3\lambda)\exp[-\theta_e^3/(9\mathrm{Ca})]\pi/2^{2/3} + O(\mathrm{Ca})$. The matching described here was investigated in greater detail for the wetting case in [16]. We found that higher order corrections in Ca were surprisingly weak, and depended only very little on the type of cutoff used at the contact line. Thus, we are confident that the same holds true in the present case.

Among all possible interface profiles near the contact line, the one with the *smallest* possible curvature (4) is of special significance, since it matches best onto the static

outer solution, whose curvature is of order one. From (4) it is seen that minimum curvature corresponds to the condition that $\mathrm{Ai}(s_1)$ must be maximal among solutions of (5). By choosing $\alpha = \alpha_{cr} \equiv -\beta \mathrm{Bi}(s_{\max})/\mathrm{Ai}(s_{\max})$ we can in fact ensure that Ai assumes its global maximum $0.535\,66\ldots$, which occurs for $s = s_{\max} = -1.0188\ldots$. Thus we have singled out a unique solution of (3) which minimizes the curvature

$$\kappa_\infty^{cr} = \frac{\mathrm{Ca}^{1/3}\theta_e}{\lambda} \frac{\exp[-\theta_e^3/(9\mathrm{Ca})]}{18^{1/3}\pi[\mathrm{Ai}(s_{\max})]^2}, \tag{7}$$

the value (7) of which increases with capillary number as expected.

Now we turn to the static part of the meniscus, which follows from (2) in the limit of vanishing speed $\mathrm{Ca} = 0$. The solution for the slope is

$$h'(x) = \theta + (\theta_{ap} - \theta)e^{-x}, \tag{8}$$

which still contains the apparent contact angle θ_{ap} as a parameter. The curvature at the contact line is $h''(0) = \theta - \theta_{ap}$; thus, the *largest* curvature θ which is physically realizable is achieved if the apparent contact angle is zero.

To construct a complete solution, we have to match the local solution near the contact line (inner solution) to the static solution (8) (outer solution). This means that the curvature κ_∞ the inner solution attains for $x/\lambda \gg 1$ must be the same as the curvature $\theta - \theta_{ap}$ of the outer solution at the position of the contact line. As illustrated in Fig. 2,

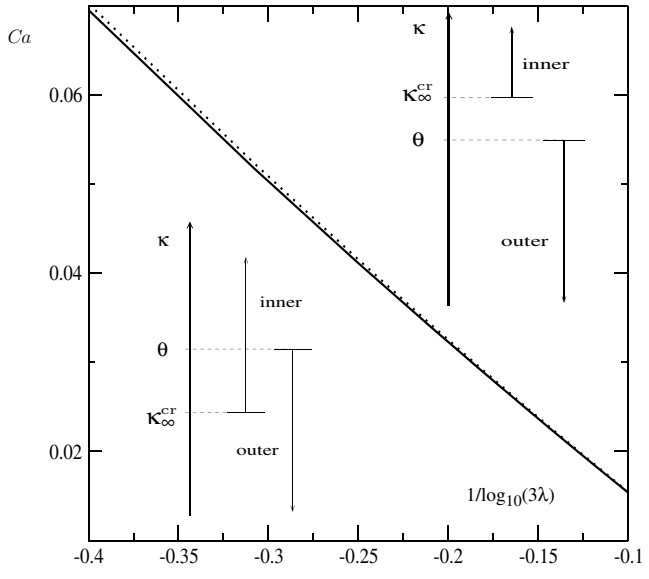

FIG. 2. The full line marks the critical capillary number Ca_{cr} above which no contact line exists, as determined by numerical integration of Eq. (2) for $\theta = \theta_e = 1$. The dashed line is the prediction of the present theory, $\kappa_\infty^{cr} = \theta$. Below Ca_{cr}, the curvature of the inner and the outer solution has an overlap region, so they can be matched. Above Ca_{cr} no such solutions exist.

for capillary numbers below a critical one there is an overlap in curvature between the two solutions. Increasing Ca above this critical value Ca_{cr}, κ_∞^{cr} rises above the maximum value θ of the curvature the outer solution can attain, and no contact line solution is possible. The critical value Ca_{cr} which separates the two regions is thus given by $\kappa_\infty^{cr} = \theta$ or

$$\mathrm{Ca}_{cr} = \frac{\theta_e^3}{9}\left[\ln\left(\frac{\mathrm{Ca}_{cr}^{1/3}\theta_e}{18^{1/3}\pi[\mathrm{Ai}(s_{\max})]^2\lambda\theta}\right)\right]^{-1}. \tag{9}$$

The critical capillary number is proportional to θ_e^3 (with a weak logarithmic correction), the constant of proportionality depending on the inclination of the plate and on the slip length. By contrast, the theory proposed by de Gennes [17] is based on the local structure of the contact line alone, and therefore misses any dependence on geometry. In a companion paper [16], we in fact show that the local contact line structure used in [17] is an artifact of the approximation being used.

For our procedure to be consistent, though, we need to make sure that the inner and the outer solution have sufficient spacial overlap to be matched. The inner and outer solutions at Ca_{cr} are, in summary, $h_{\mathrm{inner}}^{lcr} = \mathrm{Ca}_{cr}^{1/3} f(x\beta^2)$ and $h_{\mathrm{outer}}^{lcr} = \theta(1 - e^{-x})$, where f is a universal function given by the appropriate solution of (3). Thus, if $\beta^2 \gg 1$ the large-x/λ limit of h_{inner}^{lcr} overlaps with the small-x limit of h_{outer}^{lcr}, which translates into $\theta \gg \mathrm{Ca}^{1/3}$.

In Fig. 3 we show the result of a numerical integration of (2) for $\theta = 10$ at the critical capillary number. The interface slope follows the static solution perfectly almost

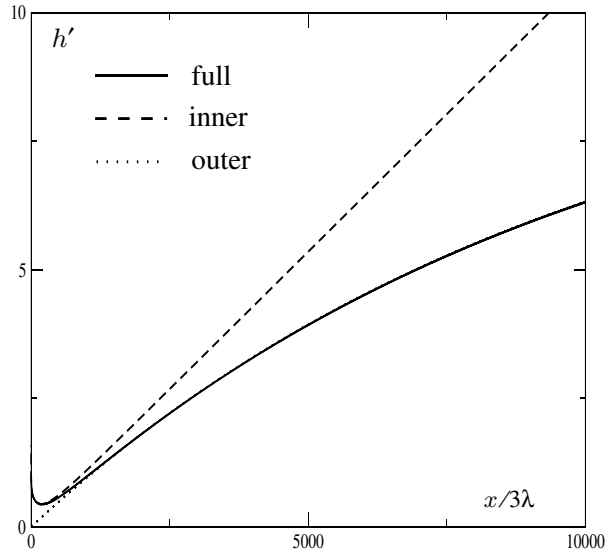

FIG. 3. A comparison of the full solution at the critical capillary number with the inner and outer solutions. We plot the slope of the interface, so $h'(0) = \theta_e = 1$ for the full solution, and $h'(0) = 0$ for the outer solution, consistent with the condition by Derjaguin and Levi. The other parameters are $3\lambda = 10^{-4}$ and $\theta = 10$, so from (9) we obtain $\mathrm{Ca}_{cr} = 0.0191$.

up to the contact line, where it has to turn over, while the static solution extrapolates to zero. Coming from the interior, the inner solution describes the full profile equally well up to the turning point. Note that there are no adjustable parameters in Fig. 3; we simply took the inner and outer solutions in the critical case. In fact, even for $\theta = 1$, when there is not yet much overlap between the inner and the outer solution, Eq. (9) already works extremely well in describing the loss of the stationary solution, as shown in Fig. 2. Again, no parameter was adjusted to achieve this comparison.

It is important to note that our approach is not limited to the moving plate geometry studied here, nor is it restricted to a specific contact line model, since it is based entirely on hydrodynamic arguments *away* from the contact line. We have used the simplest possible contact line model, assuming the microscopic contact angle to be independent of speed. If there are other sources of dissipation at the contact line, in addition to viscous dissipation in the bulk of the liquid, the microscopic angle will be effectively speed dependent [18,19]. In the dewetting case, it will be forced toward smaller values, leading to a disappearance of the contact line at smaller speeds. If, for example, van der Waals forces are dominant near the contact line [20], the slip length λ in (9) needs to be replaced by $\sqrt{A/(6\pi\gamma)}/(6\theta_e)$, which is the microscopic parameter characterizing the range of van der Waals forces. Here, A is the Hamaker constant.

To generalize to a different geometry, one has to replace (8) by the appropriate static solution for the problem at hand. This is done almost trivially for the case of a vertical wall [21], and easily extended [13] to the flow in a narrow capillary, to be able to compare directly to experiments [12]. Hocking [13] found that the present slip theory correctly predicts $\mathrm{Ca}_{cr}/\theta_e^3$ to be a constant, but overestimates this constant by a factor of 2, if reasonable values for the slip length λ are assumed. The materials used in the experiment [12] have considerable contact angle hysteresis, pointing to surface roughness. This will tend to lower the critical speed for the appearance of the Landau-Levich film [22]. New sets of experiments, using the plate geometry, are under way to clear up these questions [23].

Another important generalization is to higher dimensional problems, in which the contact line does not remain straight. An instability toward inclined contact lines was observed in [11], as well as in recent experiments with drops running down an inclined plane [24]. To explain the characteristic inclination angle of such a contact line, one needs to identify a *characteristic speed* of forced dewetting [11,25], which our present approach effectively provides.

In conclusion, in this Letter we explain the fundamental difference between a solid being withdrawn or plunging into a liquid bath. We show that the maximum capillary number for which a contact line can exist is $\mathrm{Ca}_{cr} = A\theta_e^3$, where A depends on geometry.

Special thanks are due to Petr Braun for numerous insightful discussions. Daniel Bonn and Christophe Clanet made very helpful comments on earlier versions of this manuscript.

Note added.— I very recently became aware of a paper [O.V. Voinov, J. Colloid Interface Sci. **226**, 5 (2000)], which proposes ideas similar to those of this Letter.

[1] R.V. Sedev and J.G. Petrov, Colloids Surf. **53**, 147 (1991).
[2] D. Quéré, Annu. Rev. Fluid Mech. **31**, 347 (1999).
[3] P.G. Simpkins and V.J. Kuck, J. Colloid Interface Sci. **263**, 562 (2003).
[4] L.D. Landau and B.V. Levich, Acta Physicochim. URSS **17**, 42 (1942).
[5] B.V. Derjaguin, Acta Physicochim URSS **20**, 349 (1943).
[6] C. Huh and L.E. Scriven, J. Colloid Interface Sci. **35**, 85 (1971).
[7] E.B. Dussan, V. Davis, and S.H. Davis, J. Fluid Mech. **65**, 71 (1974).
[8] L.M. Hocking, Q. J. Mech. Appl. Math. **36**, 55 (1983).
[9] P.G. de Gennes, Rev. Mod. Phys. **57**, 827 (1985).
[10] B.V. Derjaguin and S.M. Levi, *Film Coating Theory* (Focal Press, London 1964).
[11] T.D. Blake and K.J. Ruschak, Nature (London) **282**, 489 (1979).
[12] D. Quéré, C. R. Acad. Sci. Paris, Sérrie II **313**, 313 (1991).
[13] L.M. Hocking, Euro. Jnl. of Applied Mathematics **12**, 195 (2001).
[14] M. Fermigier and P. Jenffer, J. Colloid Interface Sci. **146**, 226 (1991).
[15] B.R. Duffy and S.K. Wilson, Applied Mathematics Letters **10**, 63 (1997).
[16] J. Eggers, Phys. Fluids **16**, 3491 (2004).
[17] P.G. de Gennes, Colloid Polym. Sci. **264**, 463 (1986).
[18] F. Brochard-Wyart and P.G. de Gennes, Adv. Colloid Interface Sci. **39**, 1 (1992).
[19] O.V. Voinov, Fluid Dyn. **11**, 714 (1976).
[20] P.G. de Gennes, X. Hua, and P. Levinson, J. Fluid Mech. **212**, 55 (1990).
[21] L.D. Landau and E.M. Lifshitz, *Fluid Mechanics* (Pergamon, Oxford, 1984).
[22] R. Golestanian and E. Raphaël, Europhys. Lett. **55**, 228 (2001).
[23] D. Quéré and M. Fermigier (private communication).
[24] T. Podgorski, J.M. Flesselles, and L. Limat, Phys. Rev. Lett. **87**, 036102 (2001).
[25] H.A. Stone, L. Limat, S.K. Wilson, J.M. Flesselles, and T. Podgorski, Comptes Rendus Physique **3**, 103 (2002).